

PORTLAND CEMENT ENRICHED WITH HYDROXYAPATITE FOR ENDODONTIC APPLICATIONS

**ALEXANDRA AVRAM^a, MARIA GOREA^{a,*}, REKA BALINT^a,
LUCIA TIMIS^{a,b}, STEFAN JITARU^{a,b}, AURORA MOCANU^a,
MARIA TOMOAI-COTISEL^{a,c}**

ABSTRACT Endodontic cement based on calcium silicate has been the focus of many studies. However, the quality of resulted endodontic cement needs improvement. This paper focuses on endodontic cement obtained from Portland cement enriched with two types of hydroxyapatite, simple and doped with 5% Zn. Hydroxyapatites were synthesized using a wet precipitation method and investigated by X-ray diffraction, FTIR, TEM and AFM. From a structural point of view, both hydroxyapatites were obtained in a single crystalline phase, containing particles in the nanometric range, as judged by XRD, TEM and AFM. FTIR analysis presents O-H and P-O bands specific to those in pure hydroxyapatite, confirming a hydroxyapatite lattice in both materials. Several experimental compositions of commercial Portland cement mixed with hydroxyapatite were prepared. The influence of stoichiometric and Zn doped hydroxyapatite on the resulted endodontic cement was observed in the setting time. The setting time for both cements decreased exponentially at both temperatures (22 °C and 37 °C). The normal consistency water remains constant for all experimented slurries.

Keywords: *Endodontic cement, hydroxyapatite, Zn doped hydroxyapatite, Portland cement*

^a Babeş-Bolyai University, Faculty of Chemistry and Chemical Engineering, 11 Arany J. Str., 400028, Cluj-Napoca, Romania

^b Iuliu Hațieganu University of Medicine and Pharmacy, Faculty of Dentistry, 8 Babeş V. Str., 400012, Cluj-Napoca, Romania

^c Academy of Romanian Scientists, 54 Splaiul Independentei, 050094, Bucharest, Romania

*Corresponding author: mgorea@chem.ubbcluj.ro

INTRODUCTION

Cement and ceramic-based biomaterials have been the subject of a wide number of studies regarding root repair cements, due to their properties: nontoxicity, biocompatibility, non-shrinkage, and chemical stability in biological conditions [1,2]. Their ability to chemically bond to the tooth, forming an hermetic seal, promote osseointegration, as well as having a good radiopacity have led to these material being widespread in the area of endodontics [3,4]. Endodontic bioceramics have the advantage of not being moisture or blood sensitive, therefore not being technique sensitive. When unset, they present antibacterial properties and when set, bioactive capabilities [2].

While the field of material science has produced no ideal material, synthetic hydroxyapatite (HAP, $\text{Ca}_{10}(\text{PO}_4)_6(\text{OH})_2$) has become one of the most interesting bioceramics, being similar to inorganic components from the human body [4-8]. Its ability to generate hard tissue, thus increasing the bioactivity of dental cements is of particular significance. The bioactivity of hydroxyapatite is closely related to both the type and size of the amorphous and crystalline phases present in its structure as well as in its ion release capability [9]. Due to the promising endodontic applications of hydroxyapatite, several studies have analyzed its addition to dental fillers [10].

Water-based cements have been introduced to dentistry through the use of MTA or mineral trioxide aggregate [11,12]. Broadly defined as a fine inorganic powder that has the ability to set and harden independently [13], cement is another material clinically used in dentistry. Used as filling materials, endodontic cements come in direct contact with the alveolar bone having many applications, namely: root canal fillings and sealers, apical replacement of dentine, pulp capping and root perforation repair [9,14]. Bone defects can be easily filled by the cement paste without leaving any gap between the two interfaces.

Due to its self-setting property at physiological temperatures, ample availability and lower cost, Portland cement has a long history in the reconstruction of bone defects. These materials could be an alternative to MTA, and are currently the main focus of studies in the dental fields [4,13,15,16]. This hydraulic material is mainly composed of dicalcium ($2\text{CaO}\cdot\text{SiO}_2$), and tricalcium silicate ($3\text{CaO}\cdot\text{SiO}_2$), tricalcium aluminate ($3\text{CaO}\cdot\text{Al}_2\text{O}_3$) and tetracalcium aluminoferrite ($4\text{CaO}\cdot\text{Al}_2\text{O}_3\cdot\text{Fe}_2\text{O}_3$) [17].

Portland cement has been proven to be biocompatible through previous studies that showed cements are not genotoxins [17-20]. The main component in cement, namely tricalcium silicate (C3S), has been shown to induce cell proliferation and HAP deposition on its surface [21]. Endodontic materials using a mixture of tricalcium silicate and calcium phosphates have been reported to present a modified hydration process [22].

Endodontic cements present many disadvantages, the main one being a delayed setting time, limiting its uses [23-25]. The advertised setting time of commercial endodontic cements ranges from 2 to 3 minutes (EndoChe Zr) to 4 hours (Trioxident) [15] and even 72 hours [25,26]. Given this discrepancy that can be confusing to clinicians, the influence of different additives, such as synthetic hydroxyapatite, on cement characteristics, especially setting time, is very important to know.

There are few studies on endodontic sealers with Ca and P ions release abilities and antibacterial properties [14].

Thus, our main purpose was to study the characteristics and influence of two types of synthetic hydroxyapatite, namely stoichiometric and Zn doped, on the setting time of endodontic cement.

RESULTS AND DISCUSIONS

Nanomaterials

The hydroxyapatite compositions, with and without Zn as dopant for Ca ions, are presented in Table 1.

Table 1. Composition of hydroxyapatites, stoichiometric and doped with Zn

Nanomaterial	Zn [wt%]	Ca substituted with Zn [mol%]	Theoretical formula
Stoichiometric hydroxyapatite	0	0	$\text{Ca}_{10}(\text{PO}_4)_6(\text{OH})_2$
Zn doped hydroxyapatite	5.0	7.83	$\text{Ca}_{9,217}\text{Zn}_{0,783}(\text{PO}_4)_6(\text{OH})_2$

In the experiments, the stoichiometric, uncalcined hydroxyapatite and Zn doped hydroxyapatite were mixed together with Portland cement. The compositions of endodontic cement samples are presented in Table 2.

Table 2. The studied compositions of endodontic cements

Sample/material [%]	Stoichiometric HAP	Zn doped HAP	Portland Cement
S0	-	-	100
S1	1	-	99
S2	2	-	98
S3	3	-	97
S4	5	-	95
S5	-	1	99
S6	-	2	98
S7	-	3	97

The S0 sample is composed only of Portland cement and is the standard sample. The S1, S2, S3 and S4 cements contain the various amounts of stoichiometric hydroxyapatite, while the S5, S6 and S7 cements comprise different quantities of Zn doped hydroxyapatite.

X-ray diffraction of hydroxyapatite

The X-ray diffraction (XRD) patterns of synthesized hydroxyapatite presented in Figure 1 (up) for uncalcined hydroxyapatite and in Figure 1 (down) for Zn doped hydroxyapatite, calcined at 300 °C, reveal the presence of crystalline hydroxyapatite in both samples.

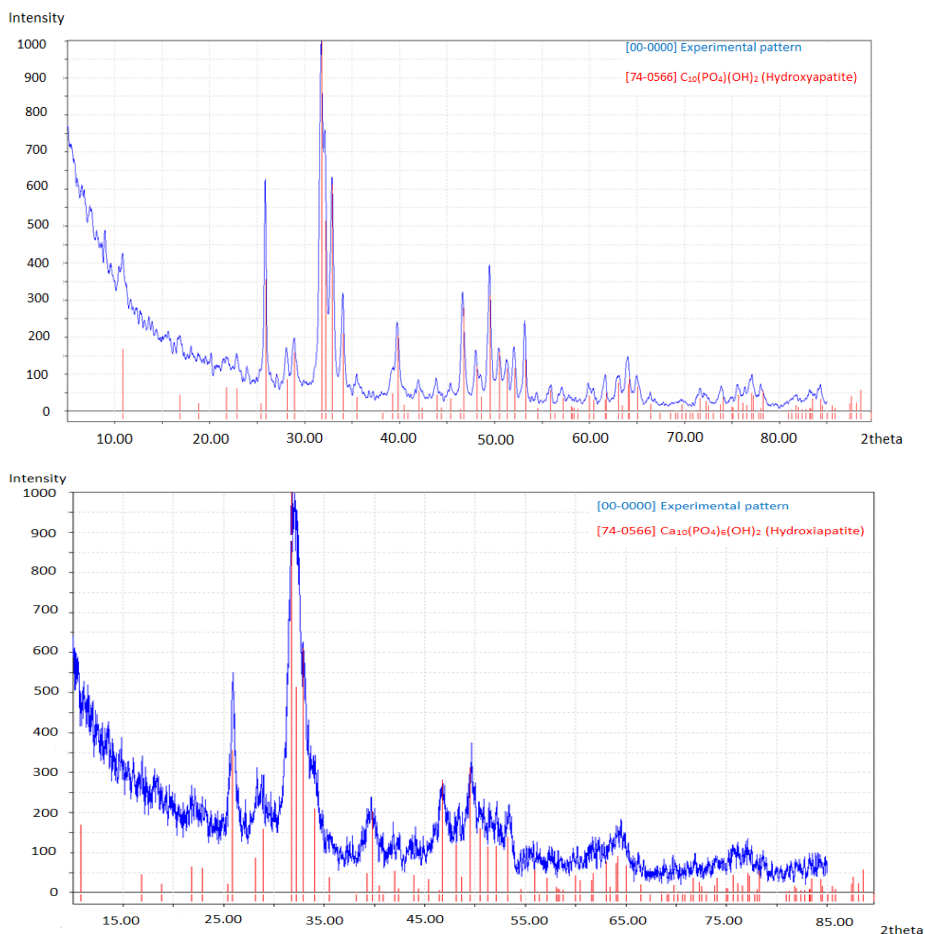


Figure 1. XRD pattern for pure, uncalcined hydroxyapatite (up) and Zn doped hydroxyapatite (down) compared with PDF 74-0566 for stoichiometric hydroxyapatite, $\text{Ca}_{10}(\text{PO}_4)_6(\text{OH})_2$.

A decrease in crystallite size and crystallinity index for Zn doped hydroxyapatite can be observed. These effects are supposedly determined by the presence of Zn ions and the sample calcination at 300 °C (Table 3).

Table 3. Crystallite sizes and crystallinity index of hydroxyapatites

Nanomaterial	Average crystallite size [nm]	Crystallinity index [%]
Stoichiometric hydroxyapatite	35.6	50.4
Zn doped hydroxyapatite	24.7	38.6

FTIR analysis for studied HAP

The FTIR spectra for both hydroxyapatite samples are presented in Figure 2. The specific vibration bands of P-O bonds from PO₄ groups can be evidenced. The peak from 962-963 cm⁻¹ appears in the apatite spectra because of the low symmetry of elemental tetrahedral cells of doped hydroxyapatite compared to free PO₄ ions from phosphates.

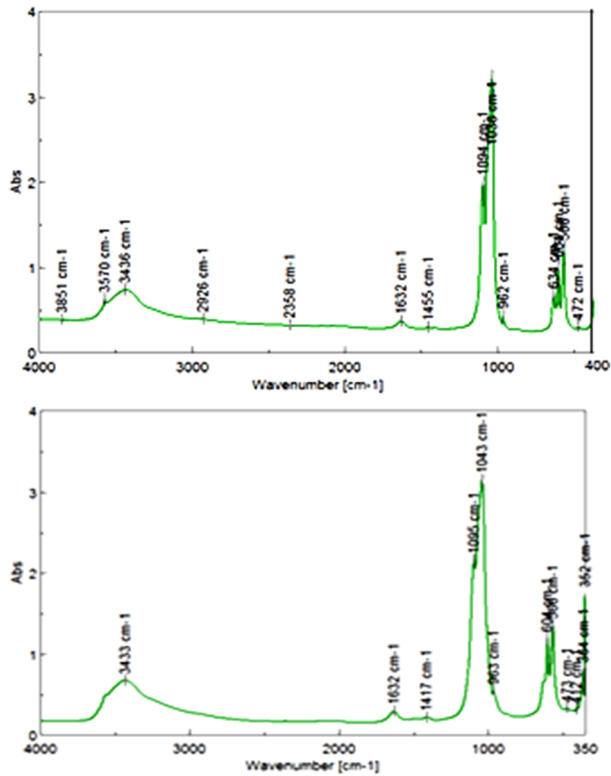


Figure 2. FTIR analysis for stoichiometric, uncalcined hydroxyapatite (up) and Zn doped hydroxyapatite calcined at 300 °C for 1h (down)

The most intense absorption band of apatite is formed from two peaks, at $1035\text{-}1044\text{ cm}^{-1}$ and $1093\text{-}1096\text{ cm}^{-1}$. The P-O asymmetric distortion is cleaved in two peaks, at 566 and $603\text{-}604\text{ cm}^{-1}$. The wide band at $3600\text{-}3300\text{ cm}^{-1}$ (with a maximum at $3420\text{-}3440\text{ cm}^{-1}$) is attributed to the O-H vibrations in the adsorbed water molecules. The narrow band at $3579\text{-}3571\text{ cm}^{-1}$, overlaid on the wide band attributed to water, is due to OH structural groups of hydroxyapatite. This observation is in accordance to the increase of water quantities in the hydroxyapatite network at a higher Zn content.

TEM images for HAP biomaterials

Transmission electron microscopy was used for investigating the morphology and size of particles in the hydroxyapatite powder (Figure 3). The image illustrates that polycrystalline hydroxyapatite with rather uniform sized particles is formed by this process. The crystallite size of hydroxyapatite measured from TEM is in the nanometric range, with a length of $40\text{-}50\text{ nm}$ and a diameter of $20\text{-}30\text{ nm}$, in accordance to XRD patterns.

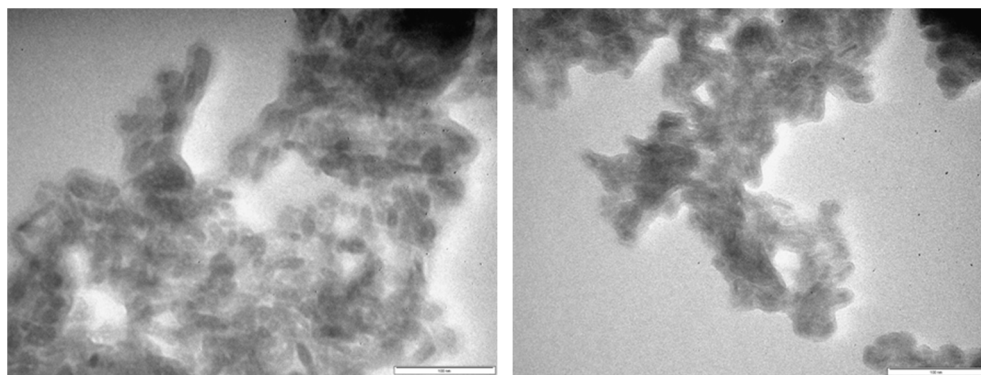


Figure 3. TEM images for stoichiometric, uncalcined hydroxyapatite (left) and Zn doped hydroxyapatite calcined at $300\text{ }^{\circ}\text{C}$ for 1h (right); 100 nm scale.

Atomic force microscopy (AFM)

AFM images and cross section profiles are given in Figure 4, for uncalcined hydroxyapatite and in Figure 5 for Zn doped hydroxyapatite, calcined at $300\text{ }^{\circ}\text{C}$ for 1h.

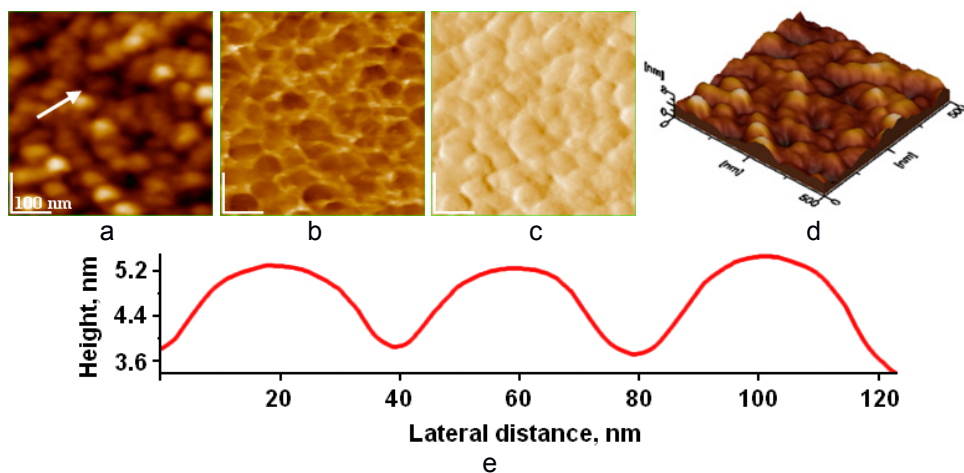


Figure 4. AFM images of HAP particles adsorbed on glass for 10 sec from aqueous dispersion: 2D topography (a), phase (b), amplitude (c), 3D- topography (d) and cross section profile (e) along the arrow in image (a); scanned area of $0.5 \mu\text{m} \times 0.5 \mu\text{m}$; average nanoparticle size of 32 nm.

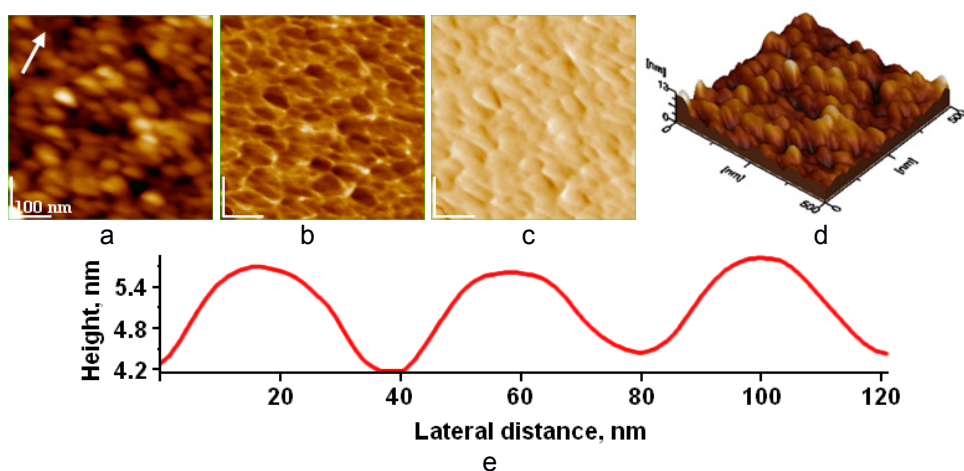


Figure 5. AFM images of HAP-5%Zn particles adsorbed on glass for 10 sec from aqueous dispersion: 2D topography (a), phase (b), amplitude (c), 3D- topography (d) and cross section profile (e) along the arrow in image (a); scanned area of $0.5 \mu\text{m} \times 0.5 \mu\text{m}$; average nanoparticle size of 27 nm.

There are mostly oblong particles, with a length of about 50 nm and diameters of 30 nm for stoichiometric hydroxyapatite and 40/20 nm for Zn doped hydroxyapatite. The size of particles is found to be in the range of 27-32 nm. These values are comparable with those determined by X-ray diffraction and SEM analysis.

Consistency water for investigated endodontic cements

Determining the normal consistency water of cement (the water quantity needed for cement slurry consistency) is an important first step towards proceeding with setting time experiments. After several trials, the normal consistency water of 87 ml for Carpat Cement Portland cement slurry was found. The predetermined consistency water for Portland cement slurry remained constant for all hydroxyapatite/cement ratios of the endodontic cements. It can be said that hydroxyapatite does not have any influence on this parameter. So, the porosity of the endodontic cement is maintained constant and, consequently, the mechanical strength.

Setting time for studied endodontic cements

The experimental data of setting time obtained from studied endodontic cements containing a consistency water of 87 ml, at temperatures of 22 °C and at 37°C, are presented in Table 4.

Table 4. Setting time of Portland cement and studied endodontic cements

Sample	Consistency water [ml]	Setting time [min]	
		at 22°C	at 37°C
S0	87	85	70
S1		70	60
S2		70	60
S3		55	45
S4		45	35
S5		70	65
S6		65	60
S7		55	45

The setting times for all experimental samples, including the standard, S0, decreases with the increasing in temperature from 22°C to 37°C, the normal body temperature. No difference can be seen through the addition of 1 and 2 wt% uncalcined hydroxyapatite (samples S1 and S2). Sample S3, containing 3 wt% hydroxyapatite, shows a more pronounced decreasing of the setting

time at both working temperatures. By increasing the hydroxyapatite content to 5 wt%, as seen in sample S4, a halving of the endodontic cement setting time can be observed. A progressive decrease of setting time in all samples containing Zn doped hydroxyapatite, namely S5, S6 and S7, can also be evidenced. Sample S7, containing 3 wt% Zn doped hydroxyapatite, shows similar behavior to that of sample S3, containing 3 wt% stoichiometric hydroxyapatite. The two types of hydroxyapatite present comparable results in the decrease of endodontic cement setting time.

CONCLUSIONS

Endodontic cements containing Portland cement and stoichiometric hydroxyapatite as well as Portland cement and Zn doped hydroxyapatite in different ratios were realized. Commercial Portland cement, having as main mineralogical components calcium silicates, was used as binder. Nanometric uncalcinated stoichiometric hydroxyapatite and Zn doped hydroxyapatite were successfully synthesized.

Quantities of 1, 2, 3 and 5 wt% of both types of hydroxyapatite were mixed with Portland cement and processed in accordance to cement standards. The workability of the cement mixtures was not influenced by adding small amounts of hydroxyapatite. The normal consistency water remains constant for all experimental slurries. The setting time for both sets of samples, with added stoichiometric, uncalcined hydroxyapatite (S1-S4) and Zn doped hydroxyapatite (S5-S7) has decreased exponentially at both working temperatures.

In conclusion, the properties, especially the setting time of studied endodontic cements obtained by adding nanometric stoichiometric and Zn doped hydroxyapatites in Portland cement mixtures can be improved. The research will continue with the testing of biological compatibility and antimicrobial activity of endodontic cements enriched with Zn doped hydroxyapatite.

EXPERIMENTAL SECTION

Materials and methods

The nanometric hydroxyapatite was prepared by the direct reaction of calcium nitrate and diammonium hydrogen phosphate at basic pH. A solution of calcium nitrate (0.25 M) was prepared by dissolving $\text{Ca}(\text{NO}_3)_2 \cdot 4\text{H}_2\text{O}$ (pure p.a., Poch S.A., Merck) in ultrapure water. Then, a 25 wt% ammonia solution was added to reach a pH of 8.5. The final solution was mixed at room temperature

with an equal volume of 0.15 M $(\text{NH}_4)_2\text{HPO}_4$ (pure p.a., Sigma-Aldrich), with pH 11 (fixed with ammonia solution). A peristaltic pump and an impact reactor type Y were used for a rapid and good homogenization. The obtained dispersion was maintained for maturation at room temperature (22 °C) for 24 h. After subsequent filtration and washing with ultrapure water (until no nitrate ions were detected), the wet precipitate was dried by lyophilization (freeze drying).

For Zn doped hydroxyapatite, a 0.25 M ($\text{Ca}^{2+} + \text{Zn}^{2+}$) solution, was prepared by dissolving the calculated amounts of $\text{Ca}(\text{NO}_3)_2 \cdot 4\text{H}_2\text{O}$ and $\text{Zn}(\text{NO}_3)_2 \cdot 6\text{H}_2\text{O}$ (from Sigma-Aldrich) in ultrapure water. The second solution was a 0.15 M PO_4^{3-} solution with L-asparagine monohydrate (purity $\geq 99.0\%$, from Merck, Germany) as surfactant. The identical processing steps were followed. The dried solid was calcined at 300 °C for one hour.

X-ray diffraction analysis was carried out using a Bruker D8 Advance diffractometer in Bragg Brentano geometry, equipped with an X-ray tube with copper K_α line and a wavelength of 1.541874 Å.

The size and morphology of hydroxyapatite crystallites were investigated by transmission electron microscopy (TEM) on a JEOL-type JEM 1010 equipment.

Atomic force microscopy analysis was carried out on a JEOL 4210 AFM apparatus, operated in tapping mode [27-35], using standard cantilevers with silicon nitride tips (resonant frequency in the range of 200–300 kHz).

Commercial Portland cement (Carpat Cement brand) as the matrix for endodontic cement mixtures was used.

Normal consistency water for investigated endodontic cements was determined following standard laboratory procedures. A quantity of 300 g cement were mixed with water ranging from 85 to 90 ml (standard for the type of Portland cement used) until a slurry was formed in the mixing bowl. The slurry was quickly poured in the mold of the Vicat apparatus and smoothed out. A 10 mm plunger was lowered to the surface of the sample and then let to fall freely. The depth was then read on the Vicat ruler. For a normal consistency, this depth should be in the 5-7 mm range.

The endodontic cement samples were prepared in a standard laboratory cement mixer. The cement and hydroxyapatite, in ratios according to Table 3, were added and homogenized for approximately 30 seconds. After this time, the water was added, the mixing continued for 1 minute on slow speed and 2 minutes on high speed, respectively. The final mixture was poured into a hard rubber truncated cone mold.

To measure the setting time of cement slurry with normal consistency water, a standard VICAT Apparatus was employed.

ACKNOWLEDGMENTS

Authors acknowledge the financial support from the Executive Agency for Higher Education, Research, Development and Innovation Funding (UEFISCDI) through grant no. 241.

REFERENCES

1. L.H. Silva Almeida, R.R. Moraes, R.D. Morgental, F.G. Pappen, *Journal of Endodontics*, **2017**, *43*, 527.
2. G. Debelian, M. Trope, *Giornale Italiano di Endodonzia*, **2016**, *30*, 70.
3. P. Bali, A.K. Shivekshith, C.R. Allamaprabhu, H.P. Vivek, *International Journal of Contemporary Dental and Medical Reviews*, **2014**, doi: 10.15713/ins.ijcdmr.17
4. F. Panahi, S.M. Rabiee, R. Shidpour, *Materials Science and Engineering C*, **2017**, *80*, 631.
5. I.R. Oliveira, T.L. Andrade, K.C.M.L. Araujo, A.P. Luz, V.C. Pandolfelli, *Ceramics International*, **2016**, *42*, 2542.
6. F. Goga, E. Forisz, A. Avram, A. Rotaru, A. Lucian, I. Petean, A. Mocanu, M. Tomoia-Cotisel, *Revista de Chimie*, **2017**, *68*, 1193.
7. J.A. Lett, M. Sundareswari, K. Ravichandran, *Materials Today: Proceedings*, **2016**, *3*, 1672.
8. S.M. Rabiee, F. Moztaazadeh, M. Solati-Hashjin, *Journal of Molecular Structure*, **2010**, *969*, 172.
9. M. Hosseinzade, R.K. Soflou, A. Valian, H. Nojehdehian, *Biomedical Research*, **2016**, *27*, 442.
10. Y.A. Moreno-Vargas, J.P. Luna-Arias, J.O. Flores-Flores, E. Orozco, L. Bucio, *Ceramics International*, **2017**, *43*, 13290.
11. J. Camilleri, F.E. Montesin, R.V. Curtis, T.R. Pitt Ford, *Dental Materials*, **2006**, *22*, 569.
12. V. Bortolotti, P. Fantazzini, R. Mongiorgi, S. Sauro, S. Zanna, *Cement and Concrete Research*, **2012**, *42*, 577.
13. K. Ishikawa, *Bioactive Ceramics: Cements*, Comprehensive Materials II, Elsevier, **2017**, 369.
14. S. Jitaru, I. Hodisan, L. Timis, A. Lucian, M. Bud, *Clujul Medical*, **2016**, *89*, 470.
15. W.N. Ha, D.P. Bentz, B. Kabler, L.J. Walsh, *Journal of Endodontics*, **2015**, *41*, 1146.
16. A.M. Negm, E.E. Hassanien, A.M. Abu-Seida, M.M. Nagy, *Experimental and Toxicologic Pathology*, **2017**, *69*, 115.
17. M.G. Gandolfi, P. Taddei, A. Tinti, E. De Stefano Dorigo, C. Prati, *Materials Science and Engineering C*, **2011**, *31*, 1412.
18. N.J. Coleman, J.W. Nicholson, K. Awosanya, *Cement and Concrete Research*, **2007**, *37*, 1518.

19. D. Araki Ribeiro, M.A. Hungaro Duarte, M. Akemi Matsumoto, M.E. Alencar Marques, D.M. Favero Salvadori, *Journal of Endodontics*, **2005**, 31, 605.
20. A. Chaipanich, P. Torkittikul, *Applied Surface Science*, **2011**, 257, 8385.
21. J. Camilleri, *Dental Materials*, **2011**, 27, 836.
22. P. Scembri-Wismayer, J. Camilleri, *Journal of Endodontics*, **2017**, 43, 751.
23. N. Wongkornchaowalit, V. Lertchirakarn, *Journal of Endodontics*, **2011**, 37, 387.
24. P. Torkittikul, A. Chaipanich, *Materials Science and Engineering C*, **2012**, 32, 282.
25. K.B. Wiltbank, S.A. Schwartz, W.G. Schindler, *Journal of Endodontics*, **2007**, 33, 1235.
26. L. Wang, X. Xie, C. Li, H. Liu, K. Zhang, Y. Zhou, X. Chang, H.H.K. Xu., *Journal of Dentistry*, **2017**, 60, 25.
27. G. Tomoaia, O. Soritau, M. Tomoaia-Cotisel, L.-B. Pop, A. Pop, A. Mocanu, O. Horovitz, L.-D. Bobos, *Powder Technology*, **2013**, 238, 99.
28. G. Tomoaia, M. Tomoaia-Cotisel, L.B. Pop, A. Pop, O. Horovitz, A. Mocanu, N. Jumate, L.-D. Bobos, *Revue Roumaine de Chimie*, **2011**, 56, 1039.
29. A. Mocanu, R. Balint, C. Garbo, L. Timis, I. Petean, O. Horovitz, M. Tomoaia-Cotisel, *Studia Universitatis Babes-Bolyai, Chemia*, **2017**, 62(2), Tom I, 95.
30. R.D. Pasca, G. Tomoaia, A. Mocanu, I. Petean, G.A. Paltinean, O. Soritau, M. Tomoaia-Cotisel, *Studia Universitatis Babes-Bolyai, Chemia*, **2015**, 60(3), 257.
31. M.A. Naghiu, M. Gorea, E. Mutch, F. Kristaly, M. Tomoaia-Cotisel, *Journal of Material Science and Technology*, **2013**, 29(7), 628.
32. G. Tomoaia, O. Horovitz, A. Mocanu, A. Nita, A. Avram, C.P. Racz, O. Soritau, M. Cenariu, M. Tomoaia-Cotisel, *Colloids and Surfaces B: Biointerfaces*, **2015**, 135, 726.
33. O. Horovitz, G. Tomoaia, A. Mocanu, T. Yupsanis, M. Tomoaia-Cotisel, *Gold Bulletin*, **2007**, 40 (4), 295.
34. M. Tomoaia-Cotisel, A. Tomoaia-Cotisel, T. Yupsanis, G. Tomoaia, I. Balea, A. Mocanu, Cs. Racz, *Revue Roumaine de Chimie*, **2006**, 51 (12), 11832.
35. P.T. Frangopol. D.A. Cadenhead, G. Tomoaia, A. Mocanu, M. Tomoaia-Cotisel, *Revue Roumaine de Chimie*, **2015**, 60(2-3), 265.